Gravitational wave production from axion rotations right after a transition to kination

Keisuke Harigaya,[1,2,3] Keisuke Inomata[ORCID],[2] and Takahiro Terada[4]

[1]*Department of Physics, University of Chicago, Chicago, Illinois 60637, USA*
[2]*Kavli Institute for Cosmological Physics and Enrico Fermi Institute, University of Chicago, Chicago, Illinois 60637, USA*
[3]*Kavli Institute for the Physics and Mathematics of the Universe (WPI), The University of Tokyo Institutes for Advanced Study, The University of Tokyo, Kashiwa, Chiba 277-8583, Japan*
[4]*Particle Theory and Cosmology Group, Center for Theoretical Physics of the Universe, Institute for Basic Science (IBS), Daejeon 34126, Korea*

Rotations of axion fields in the early Universe can produce dark matter and the matter-antimatter asymmetry of the Universe. We point out that the rotation can generate an observable amount of a stochastic gravitational wave (GW) background. It can be doubly enhanced in a class of models in which the equation of state of the rotations rapidly changes from a nonrelativistic matterlike one to a kinationlike one by (1) the so-called poltergeist mechanism and (2) slower redshift of GWs compared to the axion-kination fluid. In supersymmetric UV completion, future GW observations can probe the supersymmetry-breaking scale up to 10^7 GeV even if the axion does not directly couple to the Standard Model fields.

I. INTRODUCTION

Gravitational waves (GWs) are powerful probes of the early Universe because all the matter in the Universe can in principle produce GWs through gravitational interactions and the produced GWs are not attenuated except by cosmic expansion. For example, GWs can probe first-order phase transitions associated with spontaneous symmetry breaking (SSB) in the early Universe [1–4]. In this paper, we shed light on GWs induced by the dynamics of a Nambu-Goldstone boson arising from SSB.

Global symmetry and its SSB play important roles in solutions to the problems in the Standard Model of particle physics, including the strong *CP* problem [5,6], nonzero neutrino masses [7], and flavor hierarchies [8]. An important prediction of SSB is a Nambu-Goldstone boson [9–11]. If the symmetry is only approximate and is violated by a small amount, the boson obtains a small mass and is called a pseudo-Nambu-Goldstone boson. In particular, the boson predicted in Peccei-Quinn's solution to the strong *CP* problem is called the (QCD) axion [12,13]. Others are often called axionlike particles (ALPs), but in

this paper, we simply call any pseudo-Nambu-Goldstone bosons associated with SSB of U(1) symmetry as axions. Axions are naturally light and weakly coupled to other fields, and hence are sufficiently long-lived to be dark matter (DM) of the Universe [14–16]. Axion searches are performed and planned in a wide range of its mass and couplings to the Standard Model particles [17].

Because of the lightness, axions can exhibit interesting dynamics in the early Universe and play cosmological roles. The most commonly considered dynamics is oscillation, which may explain the observed DM abundance [14–16]. In this work, we instead consider rotation of an axion in the field space, which can be initiated by the Affleck-Dine mechanism [18] and has rich cosmological, astrophysical, and particle-physics implications [19–23]. The rotation can produce axion DM via kinetic misalignment [20,24–26], which predicts larger couplings of the axion to Standard model particles than what the conventional production mechanisms predict. The produced axion may have large density fluctuations and form mini halos [23], which can be observed through gravitational lensing [27]. The rotation can also produce the matter-antimatter asymmetry of the Universe [28]. Simultaneous production of DM and the matter-antimatter asymmetry from axion rotation strongly constrains the axion-parameter space and/or predicts signals in particle-physics experiments [21,29–36].

GW signals of the axion rotation have been discussed in the literature. Axion rotation can amplify GWs produced by quantum fluctuations during inflation or by cosmic

strings [37–39]. An axion-dark photon coupling can also produce GWs [25,40].

In this paper, we point out that the rotation itself can generate a substantial stochastic GW background through its gravitational interaction at the second order in perturbations. For a certain potential of the symmetry-breaking field, the axion rotation initially follows the equation of state of nonrelativistic matter and dominates the Universe. At some point, the equation of state suddenly changes to that of kinetic-energy-dominated fluid and, after a while, the energy density of the rotation eventually becomes subdominant compared with that of radiation [28]. The sudden transition from a matter-dominated (MD) era to a kinetic-energy-dominated (KD or kination [41–43]) era can produce strong GWs through rapid oscillations of the density perturbations with nonzero sound speed after the transition. This "poltergeist mechanism" [44,45], where a "ghost" of nonrelativistic matter produces sounds that generate GWs, has been studied for the sudden transition from a MD era to a radiation-dominated (RD) era [44–53]. GWs induced during an era with a general equation of state have been discussed in Refs. [54,55].

Throughout this paper, we take the natural unit $c = \hbar = 8\pi G = k_{\mathrm{B}} = 1$. We take the conformal Newtonian gauge,[1] in which the nonvanishing components of the metric are

$$g_{00} = -a^2(1 + 2\Phi), \quad g_{ij} = a^2\left((1 - 2\Psi)\delta_{ij} + \frac{h_{ij}}{2}\right), \quad (1)$$

where a is the scale factor, the gravitational potential Φ and the curvature perturbation Ψ are the first-order scalar perturbations, the GWs h_{ij} are the second-order tensor perturbations. We have omitted the vector perturbations and the first-order tensor perturbations because they are irrelevant to the GW production mechanism in this paper. Since we focus on the evolution of the Universe dominated by scalar fields, where the anisotropic stress vanishes [56], we set the perfect fluid condition, $\Phi = \Psi$, in the following.

II. MATTER-TO-KINATION TRANSITION AND GRAVITATIONAL WAVES

We here explain the essence of the poltergeist mechanism. The tensor perturbations in the Fourier space are induced by the scalar perturbations through [57,58]

$$h_{\boldsymbol{k}}^{\lambda\prime\prime}(\eta) + 2\mathcal{H}h_{\boldsymbol{k}}^{\lambda\prime}(\eta) + k^2 h_{\boldsymbol{k}}^\lambda(\eta) = 4S_{\boldsymbol{k}}^\lambda(\eta), \quad (2)$$

where $\boldsymbol{k}$ ($k = |\boldsymbol{k}|$) and λ denote the wave number and the polarization of the tensor perturbations, the prime is $\partial/\partial\eta$, and $\mathcal{H} = a'/a$. See also Supplemental Material (SM) [59]

for the detailed definition of the Fourier mode, $h_{\boldsymbol{k}}^\lambda$. The source term $S_{\boldsymbol{k}}^\lambda$ is given by

$$S_{\boldsymbol{k}}^\lambda = \int \frac{\mathrm{d}^3 q}{(2\pi)^3} e_{ij}^\lambda(\hat{\boldsymbol{k}}) q^i q^j \left[2\Phi_{\boldsymbol{q}}\Phi_{\boldsymbol{k}-\boldsymbol{q}} + \frac{4\hat{\Phi}_{\boldsymbol{q}}\hat{\Phi}_{\boldsymbol{k}-\boldsymbol{q}}}{3(1+w)}\right], \quad (3)$$

where $\hat{\Phi}_{\boldsymbol{k}} \equiv \mathcal{H}^{-1}\Phi_{\boldsymbol{k}}' + \Phi_{\boldsymbol{k}}$, $\hat{k} = \boldsymbol{k}/k$, $e_{ij}^\lambda(\hat{\boldsymbol{k}})$ is the polarization tensor, and $w = p/\rho$ is the equation-of-state parameter with p and ρ the pressure and the energy density, respectively. Also, for one-component fluid (no entropy perturbations), the equation of motion of Φ is given by [60]

$$\Phi''_{\boldsymbol{k}} + 3(1 + c_s^2)\mathcal{H}\Phi_{\boldsymbol{k}}' + (c_s^2 k^2 + 3(c_s^2 - w)\mathcal{H}^2)\Phi_{\boldsymbol{k}} = 0, \quad (4)$$

where c_s is the sound speed. The amplitude and the evolution of the gravitational potential Φ determine the amount of the induced GWs.

In this work, we numerically follow the evolution of Φ from a time in the MD (axion-rotation-dominated) era by solving Eq. (4) with the initial condition $\Phi = -3M\zeta/5$ and $\Phi' = 0$ even for the perturbations that enter the horizon before the MD era. The evolution of the gravitational potential before the initial time is incorporated in the factor M that depends on the scale. See SM for the concrete expression of M. Note that this initial condition is based on the assumption that the isocurvature perturbations of the axion rotation are negligible compared to the curvature perturbations.

In the poltergeist mechanism, the subhorizon perturbations that enter the horizon before the sudden transition play important roles after the transition. The gravitational potential on subhorizon scales is constant during the MD era due to the growth of the density perturbations. Once the Universe enters the era with $c_s^2 \neq 0$, the subhorizon gravitational potential starts to oscillate with the timescale $1/(c_s k)$, which can be much shorter than the Hubble timescale η. If the transition occurs suddenly, the amplitude of the gravitational potential is not much suppressed before the KD era begins. The terms $\mathcal{H}^{-1}\Phi_{\boldsymbol{k}}'(\sim\mathcal{O}(k\eta)\Phi_{\boldsymbol{k}})$ in Eq. (3) source GWs the most because of the large factor $k\eta \gg 1$. Figure 1 shows the evolution of the subhorizon gravitational potential in a concrete model that we will explain below. The case with $d = 5 \times 10^{-5}$ approximates the instantaneous transition limit, though the case with $d = 0.05$ still leads to strong GWs, as we will see below.

In addition to the poltergeist mechanism, the energy density parameter of the induced GWs is further enhanced because GWs are produced from the kination fluid that has a larger energy density than the radiation and later becomes subdominant without producing entropy.

---

[1]Though our calculation is performed in the Newtonian gauge, the final result is the gauge-independent physical contribution. This point is explained in SM in connection to the gauge-dependence issue discussed in the terada.
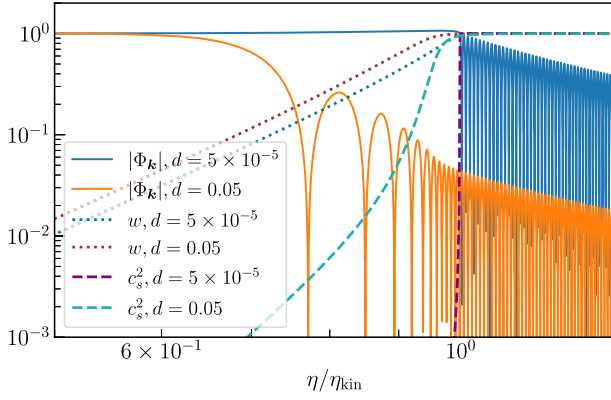
FIG. 1. The evolution of the gravitational potential in the two-field model, whose Lagrangian is given by Eq. (5). The gravitational potential is normalized so that $\Phi_k = 1$ during the MD era. We take $k\eta_{\rm kin} = 450$ for Φ_k, which is close to the nonlinear density perturbation scale during the MD era with $\mathcal{P}_\zeta = 2.1 \times 10^{-9}$ [61–63] (see also SM).

III. AXION ROTATION

A sudden change of the equation of state indeed occurs in the rotational dynamics of an axion. The axion is the angular direction θ of a complex scalar field P that has a nearly U(1)-symmetric wine-bottle potential. If the potential is flat, as naturally occurs in supersymmetric theories, it may take on a large field value in the early Universe. We further assume that the U(1) symmetry is explicitly broken by a higher-dimensional operator in the potential of P. The explicit U(1) breaking becomes effective for a large field value of P and drives angular motion [18]. Because of the cosmic expansion, the radial field value of P decreases and the higher-dimensional operator soon becomes ineffective. P continues to rotate while preserving its angular momentum in the field space, i.e., a U(1) charge. We call this motion "axion rotation".

The rotation is initially elliptic and superposition of angular motion and oscillating radial motion. The latter is dissipated via the interaction with the thermal bath. On the other hand, if the U(1) charge density is larger than $m_S T^2$ with T being the temperature of the thermal bath and m_S being the mass of the radial direction, the angular motion remains almost intact, since that is the state with the minimal free energy for a fixed U(1) charge [28,64,65].

We consider the case where the potential of P is nearly quadratic at large field values. The energy density of the Universe evolves as follows [28]. When the axion rotates at the body of the potential, the energy density decreases in proportion to a^{-3} while the radius of the rotation shrinks. Even if the Universe is initially dominated by radiation, because of the matterlike behavior, the axion rotation can dominate the Universe at $\eta = \eta_{\rm eq,1}$, which realizes the MD era. The axion reaches the bottom of the potential at $\eta = \eta_{\rm kin}$, after which the energy density decreases in

proportion to a^{-6}; the equation of state is that of kination. The axion rotation eventually becomes subdominant again at $\eta = \eta_{\rm eq,2}$ and the second (standard) RD era begins.

A concrete setup is given by a supersymmetric two-field model whose effective Lagrangian is given by [37]

$$\mathcal{L} = \left(1 + \frac{f_a^4}{16|P|^4}\right)|\partial P|^2 - m_S^2\left(|P| - \frac{(1+d)f_a^2}{4|P|}\right)^2, \quad (5)$$

where $|\partial P|^2 \equiv -g^{\mu\nu}\partial_\mu P^\dagger \partial_\nu P$, m_S is the mass parameter of the radial mode given by supersymmetry breaking, f_a is the axion decay constant, and $1 + d$ is a ratio of mass parameters in the UV completion of the model. We assume $d \geq 0$; for $d < 0$, the axion rotation is unstable [37]. The perturbativity of the model requires $f_a > m_S$. See SM for the detail. For $|P| \gg f_a$, the potential is indeed nearly quadratic.

$\eta_{\rm eq,2}$ and $\eta_{\rm kin}/\eta_{\rm eq,1}$ are related to the model parameters in Eq. (5) and the charge density normalized by the entropy density s, which we denote by $Y_\theta = 2(1 + f_a^4/(16|P|^4))|P|^2\theta'/(as)$ [37]. For $\eta_{\rm eq,2}$, we have

$$\frac{1}{2\pi\eta_{\rm eq,2}} = 1.1 \times 10^{-5}\ {\rm Hz} \times \left(\frac{T_{\rm eq,2}}{1.8 \times 10^2\ {\rm GeV}}\right), \quad (6)$$

where $T_{\rm eq,2}$ is the temperature at $\eta_{\rm eq,2}$,

$$T_{\rm eq,2} = 1.8 \times 10^2\ {\rm GeV} \times \left(\frac{f_a}{10^6\ {\rm GeV}}\right)\left(\frac{Y_\theta}{10^3}\right)^{-1}. \quad (7)$$

Consistency with the big bang nucleosynthesis (BBN) prediction requires $T_{\rm eq,2} \gtrsim 2.5$ MeV [37]. $\eta_{\rm kin}/\eta_{\rm eq,1}$ is

$$\frac{\eta_{\rm kin}}{\eta_{\rm eq,1}} = 1.7 \times 10^2 \left(\frac{m_S}{10^5\ {\rm GeV}}\right)^{\frac{1}{3}}\left(\frac{f_a}{10^6\ {\rm GeV}}\right)^{-\frac{1}{3}}\left(\frac{Y_\theta}{10^3}\right)^{\frac{2}{3}}. \tag{8}$$

Y_θ is maximized when the initial elliptic rotation has $\mathcal{O}(1)$ ellipticity, dominates the Universe, and then gets thermalized. The maximal value of Y_θ is [37]

$$Y_{\theta,\rm max} = 10^3\left(\frac{m_S}{8.7 \times 10^5\ {\rm GeV}}\right)^{-\frac{1}{3}}\left(\frac{b}{0.1}\right)^{\frac{1}{3}}, \quad (9)$$

where we have used Eq. (7) and $b \lesssim 0.1$ is a thermalization model-dependent constant.

If axion DM is produced by the rotation via the kinetic misalignment, its mass m_a is related to Y_θ as $Cm_aY_\theta \simeq 0.44$ eV [37], where C is a constant that is expected to be $\mathcal{O}(1)$ and its exact value is not yet determined. In this work, we take $C = 1$ as a reference value.

Since P is a complex field, the perturbations of P in general have two modes. However, after the oscillating radial mode is dissipated, in the limit where the rotation

is rapid, $m_S \gg \mathcal{H}/a, k/a$, one mode can be integrated out so that the perturbations are effectively those of one-component (adiabatic) fluid [37]. The equation-of-state parameter w of the axion rotation in this model is derived in Ref. [37]. We compute the sound speed of the rotation by using the adiabatic sound speed $c_s^2 = p'/\rho' = w - w'/(3\mathcal{H}(1+w))$, which is shown in Fig. 1. See also SM for the derivation of this adiabatic relation from the definition of the sound speed ($c_s^2 \equiv \delta p/\delta\rho$) for a rotating complex field. We follow the evolution of the energy density and the pressure by using the field equation and the expression of the energy momentum tensor (see SM and Ref. [37]). In Fig. 1, one can see that, for $d \ll 1$, the sound speed changes rapidly around the matter-to-kination transition. This rapid change of the sound speed is the origin of the poltergeist mechanism. $d \ll 1$ is natural when the UV theory enjoys approximate Z_2 symmetry. For convenience, we define η_{kin} as the time when $c_s^2 = 0.95$ and use this as the beginning of the KD era throughout this work. Note that the evolution of the normalized gravitational potential as a function of η/η_{kin} depends only on d and the wave number $k\eta_{\mathrm{kin}}$.

IV. SETUP

We here explain our fiducial setup. We consider a scale-invariant power spectrum for the curvature perturbations with the cutoff scales,

$$\mathcal{P}_\zeta = A\Theta(k_{\mathrm{max}} - k)\Theta(k - 1/\eta_{\mathrm{kin}}). \qquad (10)$$

We introduce an IR cutoff $1/\eta_{\mathrm{kin}}$ to reduce the computational cost by focusing on the contributions from the poltergeist mechanism, which comes from the scalar perturbations that enter the horizon during the MD era. In our fiducial parameter sets, the contributions from $k < 1/\eta_{\mathrm{kin}}$ are subdominant compared to the poltergeist contribution except on the scales much larger than the peak scale. We also introduce a UV cutoff k_{max} to obtain a conservative GW spectrum within the linear perturbation theory. Smaller-scale density perturbations enter the horizon earlier and finally become nonperturbative earlier. We take the same amplitude as the CMB fluctuations, $A = 2.1 \times 10^{-9}$, as a conservative reference value. If the axion isocurvature perturbations are not negligible or the adiabatic perturbation is highly blue-tilted, A can be larger.

For simplicity, we assume that the effective degrees of freedom is constant with $g_* = 106.75$ in $\eta_{\mathrm{eq},1} < \eta < \eta_{\mathrm{eq},2}$. Also, due to the difficulty of the numerical calculation, we only take into account the GWs induced after the KD era begins ($\eta > \eta_{\mathrm{kin}}$), which gives conservative results.

We here summarize the limitation of the linear perturbation theory, which our analysis is based on. First, the perturbations of the axion field may become nonlinear because the sudden change of the state of the Universe,

characterized by w and c_s^2, enhances higher-order perturbation contributions. Similar enhancements of the higher-order contributions have been studied in the inflation models with sharp features, which cause the sudden change of the slow-roll parameters [66–68]. We have numerically confirmed that the case of $d = 0.05$ marginally remains in the linear regime, but the case of $d = 0.01$ marginally does not. Because of this, we take $d = 0.05$ as a benchmark value. See SM for the technical details of the evaluation of the nonlinearity. In this sense, the case of $d = 5 \times 10^{-5}$ in Fig. 1 is unreliable. Nevertheless, we plot this case in Fig. 1 to show the essential idea of the sharp transition.

Second, the density perturbations that enter the horizon long before the second RD era may become nonperturbative. This is because the subhorizon density perturbation of the axion rotation, δ, grows as $\propto \ln\eta$ during the first RD era, $\propto \eta^2$ during the MD era, and $\propto \eta^{1/2}$ during the KD era, up to its oscillations. Since this growth begins after the horizon entry of the modes, the perturbations on the smallest scale k_{max} first reaches $|\delta| = 1$ if the MD era lasts long enough. If the density perturbation becomes $|\delta| > 1$, the cosmological perturbation theory is no longer reliable. On the other hand, once the induced GWs enter the horizon, they are decoupled from the source terms and freely propagating [55]. Owing to this, we can safely calculate the induced GWs on the scales that enter the horizon before the smallest-scale perturbations become $|\delta| > 1$. Technical details on our choice of k_{max} can be seen in SM.

V. RESULTS

Figure 2 shows the induced GW spectra in our setup. We can see that the induced GWs can be probed by the future observations. The peak scale is around $k_* \equiv \min[k_{\mathrm{max}}, 1/\eta_{\mathrm{eq},1}]$. The analytical estimate of the GW spectrum in $k < k_*$ is given by

$$\Omega_{\mathrm{GW}}h^2 \simeq 2 \times 10^{-11} A^2 Q^4 B(k) \frac{\eta_{\mathrm{kin}}^2}{\eta_{\mathrm{eq},1}^2} k_*^5 k\eta_{\mathrm{kin}}^6, \qquad (11)$$

where Q corresponds to the amplitude of the normalized Φ on k_* at η_{kin} (up to the oscillations), and $B(k)$ is 1 for $k > 4/\eta_{\mathrm{kin}}$ and $0.535 \times (k\eta_{\mathrm{kin}})$ for $k < 4/\eta_{\mathrm{kin}}$. The factor $\eta_{\mathrm{kin}}^2/\eta_{\mathrm{eq},1}^2 > 1$ in Eq. (11) is a redshift factor, which comes from the fact that the energy density of the rotating axion field and the induced GW are $\propto a^{-6}$ and a^{-4}, respectively. See SM for the derivation of this analytical estimate and how to numerically calculate the induced GWs, where we also extend the analyses to a general value of w.

Figure 3 shows the regions in the (m_S, f_a) plane that can be probed by the future GW experiments for given $Y_\theta/Y_{\theta,\mathrm{max}}$ with signal-to-noise ratio (SNR) > 1. See SM for how to calculate the SNR for each observation. We can see that the future observations can investigate $\mathcal{O}(10^{-1})$ GeV $\lesssim m_S \lesssim \mathcal{O}(10^7)$ GeV and $\mathcal{O}(10^2)$ GeV $\lesssim f_a \lesssim \mathcal{O}(10^8)$ GeV,
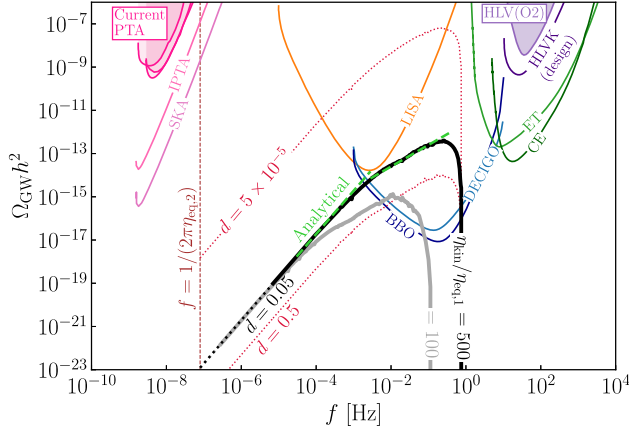
FIG. 2.   The induced GW spectrum and the sensitivities of the future and current experiments [69]. The shaded regions are excluded by the current observations. The black and gray lines are the GW spectrum with $d = 0.05$, $\eta_{eq,2} = 2 \times 10^6$ s, and different $\eta_{kin}/\eta_{eq,1}$. The curvature power spectrum is given by Eq. (10). The green dashed line shows the analytical estimate, Eq. (11), for the black-line case. The black and gray dotted lines show the region $f < 1/(2\pi \times 100\eta_{kin})$, which are superhorizon modes when the smallest-scale perturbations become nonlinear, $\delta \simeq \mathcal{O}(1)$. For comparison, the spectra for different values of d with $\eta_{kin}/\eta_{eq,1} = 500$ are shown with the red dotted lines.
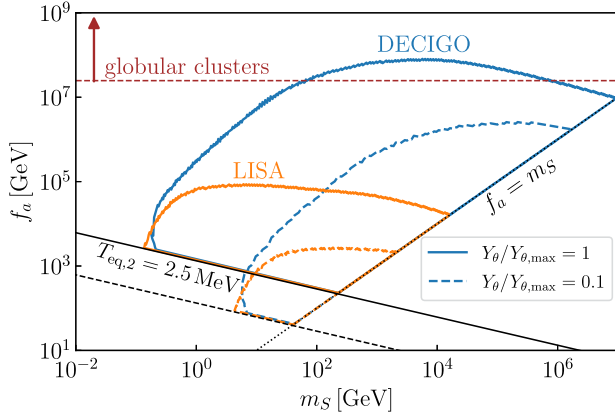
FIG. 3.   The parameter regions where LISA [4] and DECIGO [70] can probe for fixed $Y_\theta/Y_{\theta,max}$. The region surrounded by the lines realizes the SNR > 1 for each project with 1-year observation. $d = 0.05$ and $b = 0.1$ are taken for all lines. The boundaries of the BBN constraint $T_{eq,2} > 2.5$ MeV, which depends on Y_θ, and the perturbativity constraint $f_a > m_S$ are shown by black lines. BBO has a similar sensitivity as DECIGO. Other projects in Fig. 2 do not have a region with SNR > 1. The parameter region below the horizontal brown line is constrained from globular clusters [71] if the coupling between axion and photon is given by $g_{a\gamma\gamma} = \alpha/(2\pi f_a)$ with α the fine structure constant.

depending on the value of $Y_\theta/Y_{\theta,max}$. Note that these parameter regions are testable even if the axion is not coupled to the photon.

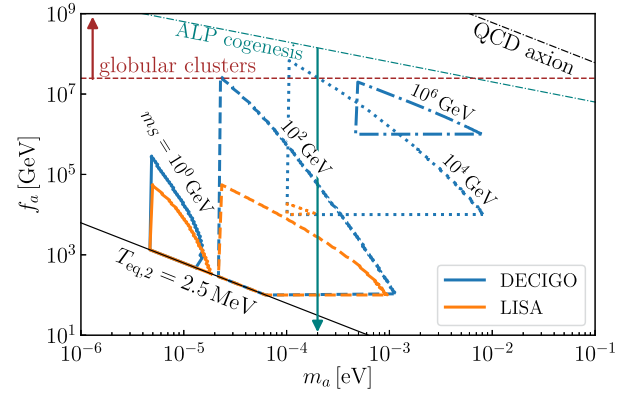Figure 4 shows the observable regions in the (m_a, f_a) plane for given m_S when the axion DM is produced from

FIG. 4.   The regions in the $m_a - f_a$ plane with fixed m_S that can be probed by future GW observations with SNR > 1 when axion DM is produced from the rotation. The prediction of the QCD axion and the ALP cogenesis are also shown. For the ALP cogenesis, the region below the line is the prediction. See the caption of Fig. 3 for the explanation on the other lines.

the rotation. The horizontal and vertical cuts in the observable regions come from the constraints $f_a > m_S$ and $Y_\theta < Y_{\theta,max}$, respectively. The black dot-dashed line is the prediction of the QCD axion and the region below the dark-cyan dot-dashed line is the prediction of the scenario where the matter-antimatter asymmetry of the Universe is generated by the axion rotation and the electroweak-sphaleron process, called ALP cogenesis [21].

VI. SUMMARY AND DISCUSSION

In this paper, we have pointed out that axion rotation can produce strong GWs by the poltergeist mechanism through the sudden transition from a MD era to a KD era. The produced GWs may be abundant enough to be detected by future GW observations. These GW signals do not rely on the coupling of the axion to the Standard Model particles and therefore enable us to investigate the uncharted parameter region of axion models. The mass of the U(1) symmetry-breaking field is given by supersymmetry breaking, and GW observations can probe supersymmetry-breaking scale as high as 10^7 GeV.

The poltergeist mechanism in our setup is realized by the approximately homogeneous one-component fluid (i.e., the axion rotation) whose equation of state changes rapidly. This is advantageous compared to the existing examples of the poltergeist mechanism, which are based on the simultaneous evaporation of localized objects such as black holes. In such cases, the distributions of mass and spin must be sufficiently narrow [45]. Our scenario is free from this issue and thus more robust against cosmological/astrophysical uncertainties.

We also mention possible extensions of this work. 1) We neglected the contributions from nonlinear density fluctuations by introducing k_{max} in this work, but they may produce non-negligible GWs. Since these GWs cannot

be calculated within the linear perturbation theory, we need to calculate them with a nonperturbative method, such as lattice simulations and the N-body simulations [72]. See also Refs. [73,74] for earlier attempts. 2) When the curvature power spectrum is enhanced on small scales or the isocurvature perturbations of the axion rotation are large, an observable amount of GWs can be produced in a wider class of cosmological histories and axion models. If the matter-to-kination transition is sudden and the axion rotation dominates for a long period, the poltergeist mechanism dominantly produces GWs and our analysis in this paper is applicable just by increasing A, though the cutoff k_{max} becomes smaller because the density perturbations reach unity within a shorter time period after its horizon entry. Even if the transition is not so sudden, or the axion rotation domination occurs only for a short period or does not occur at all, strong GWs can still be induced because of the large density perturbations. Computation of the GW spectrum for these cases, especially for the no-axion-domination case, requires careful calculation of the evolution of the density perturbations of the two fluids, axion and radiation. 3) The large axion isocurvature perturbations can also produce primordial black holes via the collapse of large fluctuations. During the axion-dominated era, the large axion isocurvature perturbations become the curvature perturbations and PBHs can be produced from the large curvature perturbations. In our scenarios, the first part of the axion-dominated era is a MD era and the PBH production rate is enhanced during the MD era due to the absence of the pressure in fluid [75–78]. This would result in the increase of the PBH abundance only within the mass range that corresponds to the horizon scales during the MD era. Investigations for these topics are left for future work.

[1] C. Caprini *et al.*, J. Cosmol. Astropart. Phys. 04 (2016) 001.

[2] C. Caprini and D. G. Figueroa, Classical Quantum Gravity **35**, 163001 (2018).

[3] C. Caprini *et al.*, J. Cosmol. Astropart. Phys. 03 (2020) 024.

[4] P. Auclair *et al.* (LISA Cosmology Working Group), Living Rev. Relativity **26**, 5 (2023).

[5] R. D. Peccei and H. R. Quinn, Phys. Rev. Lett. **38**, 1440 (1977).

[6] R. D. Peccei and H. R. Quinn, Phys. Rev. D **16**, 1791 (1977).

[7] Y. Chikashige, R. N. Mohapatra, and R. D. Peccei, Phys. Lett. **98B**, 265 (1981).

[8] C. D. Froggatt and H. B. Nielsen, Nucl. Phys. **B147**, 277 (1979).

[9] Y. Nambu and G. Jona-Lasinio, Phys. Rev. **122**, 345 (1961).

[10] J. Goldstone, Nuovo Cimento **19**, 154 (1961).

[11] J. Goldstone, A. Salam, and S. Weinberg, Phys. Rev. **127**, 965 (1962).

[12] S. Weinberg, Phys. Rev. Lett. **40**, 223 (1978).

[13] F. Wilczek, Phys. Rev. Lett. **40**, 279 (1978).

[14] J. Preskill, M. B. Wise, and F. Wilczek, Phys. Lett. **120B**, 127 (1983).

[15] L. F. Abbott and P. Sikivie, Phys. Lett. **120B**, 133 (1983).

[16] M. Dine and W. Fischler, Phys. Lett. **120B**, 137 (1983).

[17] C. B. Adams *et al.*, arXiv:2203.14923.

[18] I. Affleck and M. Dine, Nucl. Phys. **B249**, 361 (1985).

[19] K. Kamada and C. S. Shin, J. High Energy Phys. 04 (2020) 185.

[20] R. T. Co, L. J. Hall, and K. Harigaya, Phys. Rev. Lett. **124**, 251802 (2020).

[21] R. T. Co, L. J. Hall, and K. Harigaya, J. High Energy Phys. 01 (2021) 172.

[22] R. T. Co, K. Harigaya, and A. Pierce, J. Cosmol. Astropart. Phys. 10 (2022) 037.

[23] C. Eröncel and G. Servant, J. Cosmol. Astropart. Phys. 01 (2023) 009.

[24] R. T. Co, L. J. Hall, K. Harigaya, K. A. Olive, and S. Verner, J. Cosmol. Astropart. Phys. 08 (2020) 036.

[25] R. T. Co, K. Harigaya, and A. Pierce, J. High Energy Phys. 12 (2021) 099.

[26] C. Eröncel, R. Sato, G. Servant, and P. Sørensen, J. Cosmol. Astropart. Phys. 10 (2022) 053.

[27] A. Arvanitaki, S. Dimopoulos, M. Galanis, L. Lehner, J. O. Thompson, and K. Van Tilburg, Phys. Rev. D **101**, 083014 (2020).

[28] R. T. Co and K. Harigaya, Phys. Rev. Lett. **124**, 111602 (2020).

[29] R. T. Co, N. Fernandez, A. Ghalsasi, L. J. Hall, and K. Harigaya, J. High Energy Phys. 03 (2021) 017.

[30] K. Harigaya and I. R. Wang, J. High Energy Phys. 10 (2021) 022; 12 (2021) 193(E).

[31] S. Chakraborty, T. H. Jung, and T. Okui, Phys. Rev. D **105,** 015024 (2022).

[32] J. Kawamura and S. Raby, J. High Energy Phys. 04 (2022) 116.

[33] R. T. Co, K. Harigaya, Z. Johnson, and A. Pierce, J. High Energy Phys. 11 (2021) 210.

[34] P. Barnes, R. T. Co, K. Harigaya, and A. Pierce, J. High Energy Phys. 05 (2023) 114.

[35] R. T. Co, V. Domcke, and K. Harigaya, J. High Energy Phys. 07 (2023) 179.

[36] M. Badziak and K. Harigaya, J. High Energy Phys. 06 (2023) 014.

[37] R. T. Co, D. Dunsky, N. Fernandez, A. Ghalsasi, L. J. Hall, K. Harigaya, and J. Shelton, J. High Energy Phys. 09 (2022) 116.

[38] Y. Gouttenoire, G. Servant, and P. Simakachorn, arXiv:2108 .10328.

[39] Y. Gouttenoire, G. Servant, and P. Simakachorn, arXiv:2111 .01150.

[40] E. Madge, W. Ratzinger, D. Schmitt, and P. Schwaller, SciPost Phys. **12,** 171 (2022).

[41] B. Spokoiny, Phys. Lett. B **315,** 40 (1993).

[42] M. Joyce, Phys. Rev. D **55,** 1875 (1997).

[43] P. G. Ferreira and M. Joyce, Phys. Rev. D **58,** 023503 (1998).

[44] K. Inomata, K. Kohri, T. Nakama, and T. Terada, Phys. Rev. D **100,** 043532 (2019).

[45] K. Inomata, M. Kawasaki, K. Mukaida, T. Terada, and T. T. Yanagida, Phys. Rev. D **101,** 123533 (2020).

[46] G. White, L. Pearce, D. Vagie, and A. Kusenko, Phys. Rev. Lett. **127,** 181601 (2021).

[47] G. Domènech, C. Lin, and M. Sasaki, J. Cosmol. Astropart. Phys. 04 (2021) 062; 11 (2021) E01.

[48] G. Domènech, V. Takhistov, and M. Sasaki, Phys. Lett. B **823,** 136722 (2021).

[49] K. D. Lozanov and V. Takhistov, Phys. Rev. Lett. **130,** 181002 (2023).

[50] N. Bhaumik, A. Ghoshal, and M. Lewicki, J. High Energy Phys. 07 (2022) 130.

[51] N. Bhaumik, A. Ghoshal, R. K. Jain, and M. Lewicki, J. High Energy Phys. 05 (2023) 169.

[52] S. Kasuya, M. Kawasaki, and K. Murai, J. Cosmol. Astropart. Phys. 05 (2023) 053.

[53] G. Domènech and M. Sasaki, Classical Quantum Gravity **40,** 177001 (2023).

[54] G. Domènech, Int. J. Mod. Phys. D **29,** 2050028 (2020).

[55] G. Domènech, S. Pi, and M. Sasaki, J. Cosmol. Astropart. Phys. 08 (2020) 017.

[56] S. Weinberg, *Cosmology* (Oxford University Press, New York, 2008).

[57] K. N. Ananda, C. Clarkson, and D. Wands, Phys. Rev. D **75,** 123518 (2007).

[58] D. Baumann, P. J. Steinhardt, K. Takahashi, and K. Ichiki, Phys. Rev. D **76,** 084019 (2007).

[59] See Supplemental Material at http://link.aps.org/ supplemental/10.1103/PhysRevD.108.L081303 not only for the definition of the Fourier mode of the tensor perturbations, but also for a review of equations of motion for a rotating field and two-field model, the detailed calculation of the evolution of the background and perturbation quantities, and induced GWs, and the discussion on the limitation of the linear analysis.

[60] V. Mukhanov, *Physical Foundations of Cosmology* (Cambridge University Press, Cambridge, England, 2005).

[61] H. Assadullahi and D. Wands, Phys. Rev. D **79,** 083511 (2009).

[62] K. Kohri and T. Terada, Phys. Rev. D **97,** 123532 (2018).

[63] K. Inomata, K. Kohri, T. Nakama, and T. Terada, J. Cosmol. Astropart. Phys. 10 (2019) 071.

[64] M. Laine and M. E. Shaposhnikov, Nucl. Phys. **B532,** 376 (1998).

[65] V. Domcke, K. Harigaya, and K. Mukaida, J. High Energy Phys. 08 (2022) 234.

[66] P. Adshead and W. Hu, Phys. Rev. D **89,** 083531 (2014).

[67] K. Inomata, E. McDonough, and W. Hu, Phys. Rev. D **104,** 123553 (2021).

[68] K. Inomata, E. McDonough, and W. Hu, J. Cosmol. Astropart. Phys. 02 (2022) 031.

[69] K. Schmitz, J. High Energy Phys. 01 (2021) 097.

[70] S. Kawamura *et al.*, Prog. Theor. Exp. Phys. **2021,** 05A105 (2021).

[71] M. J. Dolan, F. J. Hiskens, and R. R. Volkas, J. Cosmol. Astropart. Phys. 10 (2022) 096.

[72] M. Kawasaki and K. Murai, arXiv:2308.13134.

[73] K. Jedamzik, M. Lemoine, and J. Martin, J. Cosmol. Astropart. Phys. 09 (2010) 034.

[74] K. Jedamzik, M. Lemoine, and J. Martin, J. Cosmol. Astropart. Phys. 04 (2010) 021.

[75] M. Yu. Khlopov and A. G. Polnarev, Phys. Lett. **97B,** 383 (1980).

[76] A. G. Polnarev and M. Yu. Khlopov, Sov. Astron. **26,** 9 (1982).

[77] T. Harada, C.-M. Yoo, K. Kohri, K.-i. Nakao, and S. Jhingan, Astrophys. J. **833,** 61 (2016).

[78] T. Harada, C.-M. Yoo, K. Kohri, and K.-I. Nakao, Phys. Rev. D **96,** 083517 (2017).